Lawrence Berkeley National Laboratory

Lawrence Berkeley National Laboratory

Title

Induced polarization response of microbial induced sulfide precipitation

Permalink

https://escholarship.org/uc/item/3n14p5tk

Authors

Ntarlagiannis, Dimitrios
Williams, Kenneth Hurst
Slater, Lee
et al.

Publication Date

2004-06-04

Peer reviewed

Induced polarization response of microbial induced sulfide precipitation

Dimitrios Ntarlagiannis[1*], Kenneth Hurst Williams[2,3], Lee Slater[1] and Susan Hubbard[3]

[1]Department of Earth & Environmental Sciences, Rutgers University, Newark, NJ 07102

[2]Department of Environmental Science, University of California at Berkeley, Berkeley, CA 94720

[3]Lawrence Berkeley National Laboratory, 1 Cyclotron Rd. MS-90-1116, Berkeley, CA 94720

[*] corresponding author

Abstract

A laboratory scale experiment was conducted to examine the use of induced polarization and electrical conductivity to monitor microbial induced sulfide precipitation under anaerobic conditions in sand filled columns. Three columns were fabricated; one for electrical measurements, one for geochemical sampling and a third non-inoculated column was used as a control. A continual upward flow of nutrients and metals in solution was established in each column. *Desulfovibrio vulgaris* microbes were injected into the middle of the geochemical and electrical columns. Iron and zinc sulfides precipitated along a microbial action front as a result of sulfate reduction due by *Desulfovibrio vulgaris*. The precipitation front initially developed near the microbial injection location, and subsequently migrated towards the nutrient inlet, as a result of chemotaxis by *Desulfovibrio vulgaris*. Sampling during and subsequent to the experiment revealed spatiotemporal changes in the biogeochemical measurements associated with microbial sulfate reduction. Conductivity measurements were insensitive to all biogeochemical changes occurred within the column. Changes in the IP response (of up to 14 mrad) were observed to coincide in place and in time with the active microbe respiration / sulfide precipitation front as determined from geochemical sampling. The IP response is correlated with the lactate concentration gradient, an indirect measurement of microbial metabolism, suggesting the potential of IP as a method for monitoring microbial respiration / activity. Post experimental destructive sample analysis and SEM imaging verified the geochemical results and supported our hypothesis that microbe induced sulfide precipitation is directly detectable using electrical methods. Although the processes not fully understood, the IP response appears to be sensitive to this anaerobic microbial precipitation, suggesting a possible novel application for the IP method.

Introduction

In anoxic environments and under low temperatures (i.e. <100°C) the most kinetically favorable mechanism by which sulfide is produced is through dissimilatory sulfate reduction by bacteria. Although environmental conditions may be highly variable, it is commonly accepted that the activity of sulfate reducing bacteria are directly responsible for the formation of sulfide minerals, particularly in marine environments and wetlands. Such microbial induced precipitation mechanisms are of vital importance for environmental purposes as they help regulate the cycling of such elements such as iron and sulfur and may be essential in the remediation of mine wastes using natural or artificial wetlands. Moreover, the large stratiform sphalerite ore deposits, in the early formation stages, may have been mediated by microorganisms under similar processes (Labrenz et al. 2000).

The induced polarization (IP) method is a non-invasive method for probing the physical and chemical characteristics of the mineral-fluid interface in soils and rocks. In metallic mineral containing rocks the IP response is associated with the development of ionic concentration gradients that result from flow of redox-active and inactive ions between the solution and the metal mineral surface (Wong 1979). The redox active ions facilitate electron transfer at the metal surface, allowing electric current to bridge the energy barrier between electrolytic and electronic current flow (Angoran and Madden 1977; Marshall and Madden 1959). IP has been successfully used to explore for economically viable disseminated sulfide deposits (Marshall and Madden 1959; Pelton et al. 1978; Sumner 1976; Vanhala 1997) and is capable of resolving as low as

1% metal sulfide concentration. Wong (1979) presented an electrochemical model for predicting the IP response of disseminated metal sulfide ores at low (up to 16% by volume) metal concentrations.

We can represent the low-frequency electrical properties by a complex conductivity (σ^*). At low frequencies (< 1 kHz) we assume $\sigma^* = \sigma_{el} + \sigma^*_{int}$, where σ_{el} is a real-valued term representing the conductivity of the electrolytic current path through the interconnect pore space. The σ_{el} is strongly dependent on the conductivity of the electrolyte (σ_w) and given by $\sigma_{el} = \sigma_w/F$, where F represents a formation factor (Archie 1942). The complex term σ^*_{int} accounts for interfacial charge transport within the system and contains both ohmic (σ'_{int}) and polarization (σ''_{int}) terms. The σ^*_{int} will contain contributions from any IP mechanisms: in the experiments described here we assume that the movement of ions to/from metallic mineral surfaces is the dominant IP effect. We measure two system parameters, which we represent either as the real (σ') and imaginary (σ'') parts of the system response, or the conductivity magnitude ($|\sigma|$) and phase (φ). The real part is a function of both electrolytic and interfacial charge transport $\sigma' = \sigma_{el} + \sigma'_{int}$, whereas the imaginary part results exclusively from the interfacial ion transport mechanisms $\sigma'' = \sigma''_{int}$ and is the IP effect. For most IP effects (φ<100 mRad) the conductivity magnitude ($|\sigma|$) is dominated by σ' and $\varphi = \sigma''/\sigma'$.

Our experiment was motivated by the possibility of using IP to remotely detect and monitor microbial sulfate precipitation. We report here IP measurements on a column experiment that was loosely based on replicating environmental conditions reported in Labrenz et al. (2000), who worked with natural samples from a flooded mine. We present the results of IP measurements in a system undergoing active microbial metabolism, electron shuttling and resulting metal sulfide precipitation. Our results demonstrate the potential of IP in monitoring microbial hosted metal sulfide precipitation.

Methods

The experiment involved the precipitation of iron and zinc sulfides due to microbial action under anaerobic conditions. Three columns were fabricated; one for electrical measurements, one for geochemical sampling and a third non-inoculated column was used as a control. Figure [1] shows the active columns from which electrical and geochemical measurements were obtained. Each column was 30.5 cm in length with a 5.08 cm diameter. Electrical measurements of $|\sigma|$ and φ were made with a NI 4551 two channel dynamic signal analyzer (DSA) as described elsewhere (Slater and Lesmes 2002). Non-polarizing Ag-AgCl electrodes were placed 3.5 cm apart in chambers just on the edge of the sample to minimize spurious polarization that can develop at the electrode surface (Vanhala and Soininen 1995). Gold current injection electrodes were placed at either end of the column. On the geochemical sampling column, seven sampling ports were placed with 3.8 cm separation starting from the column base. Sampling ports on the geochemical column coincided with each electrode pair on the electrical column (Figure 1).

Each column was packed with standard 20-30 mesh silica sand (Ottawa, Il) composed of 99.8% quartz and 0.2% magnetite with grain size varying from 600µm up to 800µm (specific surface area 1.1-2.0 m2/g). Nutrients and metals in solution were then circulated through each column. The saturating fluid was composed of 2.8mM lactate, 4.0mM sulfate, 0.31mM soluble zinc and 0.36mM soluble iron with inflow from the bottom and a velocity of 50 cm/day over the course of the experiment. The electrical conductivity of the circulating fluid (σ_w) was maintained at 1300µS/cm ±75 µS/cm (+/- 50µS/cm conductivity meter accuracy) for the duration of the experiment. The bacterium chosen for the experiment was *Desulfovibrio vulgaris*, a common soil borne and aquifer microorganism that the US Department of Energy is currently investigating for its use in facilitating bioremediation. Bacterial injection was performed with a syringe thorough the top end of the columns, with the injection point close to the middle of the columns, or between electrode pair 4-5 in the electrical column and proximal to sampling port 3 in the geochemical column.

Geochemical sampling included sulfate, acetate, lactate, zinc and iron concentration in solution, as well as biomass counts. Sulfate, lactate and acetate concentration were measured using ion chromatography method, and Fe and Zn analysis was performed using ICP-AES. Sampling was performed from the sampling column (ports + effluent) as well as the effluent of the electrical and control columns. During the first month of the experiment, geochemical sampling and electrical measurements were performed two – three times a week (for both columns) with a reduced frequency thereafter. Sampling on both columns was performed either on the same day or on immediately consecutive days. All results were compared to the non-inoculated column, which showed no change in any of the measured parameters throughout the column. Upon completion of the experiment, destructive analysis and SEM imaging was performed. Post

destructive analysis and imaging was utilized to assess the sediment affixed cell densities throughout the column and to investigate the spatial relationship between sulfide precipitates and microbes.

Results

Figure 2 shows the conductivity magnitude ($|\sigma|$) and phase (φ) response observed between electrode pairs 1-2, 3-4, 4-5 and 6-7. In all cases, we plot the measurements recorded at 35 Hz. The responses between pair 5-6 and 7-8 are not shown for brevity but are essentially identical to that observed between pair 6-7. Similarily, the responses associated with pair 2-3 are identical to those associated with pair 3-4. We also schematically show the IP column summarizing location of electrode pairs relative to zones of bacteria injection and final bacterial accumulation. We first note that $|\sigma|$ shows no systematic variation through the duration of the experiment. The variation in the conductivity for the period of the experiment is small and most likely associated with variability in σ_w of the circulating fluid. The φ between electrode pairs 5-6 and 6-7, away from the zone of microbial activity, also remains essentially constant throughout the experiment.

The zones of bacterial injection and final bacterial accumulation are both characterized by the development and later recession of a distinctive phase anomaly. At the zone of bacterial injection between electrode pairs 4-5 we observe an increase in φ after four days with a maximum of 6 mrad recorded on day 10. The φ then recedes from day 12 to the end of the experiment and background φ values were obtained by day 48. The response observed between electrode pairs 1-2 (just above the zone of final bacterial accumulation) is similar to that recorded between electrode pairs 4-5. However, the responses near the nutrient inlet differ from those near the bacterial injection location by several factors: (a) the maximum φ anomaly is greater, reaching 14 mrad; (b) the onset of the φ increase occurs somewhere between 6-8 days later than in the zone of bacterial injection; (c) the recession of the φ anomaly is initially steeper than that recorded in the zone of bacterial injection, but then levels off and does not return to background levels within the duration of the experiment (a) 3 mrad anomaly is still observable after 48 days). In between the zones of bacterial injection and final accumulation, electrode pair 3-4 exhibits only a very subtle response over the duration of the experiment. A small (approximately -1 mrad) φ anomaly occurs around day 6. We note that a similar anomaly (- 1.5 mrad) immediately precedes (recorded on day 10) the sharp rise in the φ observed between electrode pairs 1-2 immediately above the zone of final bacterial accumulation.

Discussion

Our data indicate a distinctive temporal IP response that develops during microbial mediated metal sulfide precipitation. In our discussion we address the issue of the source mechanism of this IP signature and its relationship to microbial processes occurring within the column. As previously discussed, IP is a well proven tool for detecting metal sulfide minerals disseminated throughout a rock unit. As such, we then anticipate that the formation of metal sulfide shells on microbes within the sand columns might generate detectable IP signatures. Post destructive analysis of the inoculated columns confirmed that sulfide formation was associated with bacterial cells. Figure [3] shows two SEM images of samples taken from the IP column, one [3a] from the upper region of the column near electrode pair 6-7 and one [3b] from the zone of final bacterial accumulation below electrode pair 1-2. Figure [3a] shows a single viable microbial cell that is encrusted with sulfide nodules; the presence of a flagellum suggests the microbe is still motile even given the presence of the sulfide coating. Figure [3b] shows a quartz grain encrusted with a thick layer of metal-sulfide coated bacterial cells forming a dense biofilm; both images show the effect of metal precipitation on bacteria cells resulting from sulfate reduction.

The IP response has a distinct temporal character, such that the anomaly has dissipated by the end of monitoring. Valuable insight into the source of the IP signature comes from analysis of the geochemical data. Figure 4a shows the sulfate and lactate concentration of sampling ports 5 (bacterial injection) and 1 (final bacterial accumulation). Decreases in the lactate and sulfate concentration in the fluid over time are indicative of bacterial metabolism and cell respiration (Madigan et al. 1997), both of which are attributes that can be used as an indirect measure of microbial action in the column and of the areas with high bacterial populations. Initial sulfate/lactate consumption occurs primarily close to the zone of bacterial injection. For the first few days after injection no changes are observed as bacteria adjust to the new geochemical conditions (phase lag). The sulfate/lactate consumption starts after 4 days at port 4 (bacterial injection) and lactate is entirely depleted at this location after 10 days. At port 1 the sulfate/lactate consumption occurs after about 15 days but is never completely depleted due to continual replenishment

from the influent. This temporal shift of the zone of lactate reduction towards the influent is attributed to the chemotactic mobility of *Desufovibrio. vulgaris* towards areas with higher substrate concentrations that act as attractant (Madigan et al. 1997)

Figure 4b shows the gradient of the lactate concentration as a function of time at the zone of microbial injection and the zone of final microbial accumulation. The rate of lactate consumption is indicative of the rate of microbial metabolism and cell respiration. The φ response observed in the zone of microbial injection (electrode pair 4-5) and zone of final bacterial accumulation (electrode pair 1-2) is re-plotted to facilitate comparison. This plot reveals considerable similarity between the shape of the lactate consumption rate and the phase anomaly. Intriguingly, this dataset suggests that the IP response is proportional to the rate of microbial metabolism and metal sulfide precipitation. Although we cannot conclusively isolate the exact cause of the IP response, we suggest that it is the formation of the metal sulfide shells on the bacteria and resulting polarization enhancement as predicted by the model proposed by Wong (1979). As a result of sulfate respiration, iron and zinc sulfides precipitate on the bacteria cell forming a metallic coating on the outer cell wall. The magnitude of the IP response is proportional to the surface area of metal sulfide in contact with solution. The IP response can thus be attributed to the development of large metal sulfide surface areas during microbial metabolism, as inferred from the SEM images (figure 3). We also suggest that the IP mechanism might in part be related to the electron shuttling between the fluid and mineral phase that is facilitated by cell metabolism and respiration. During microbial metabolism bacterial cells act as ion-penetrable membranes to redox active (reducible) ions in solution. In our experiment, the bacterial cells are permeable to sulfate ions in solution. Ionic diffusion through the cells might be enhanced during application of an external electric field and add to the IP response. Both mechanisms support the observation of a later relaxation in the ϕ as the IP behavior is intimately related to the concentration of respiring cells that move towards the nutrient inlet under the chemotactic gradients.

Two issues arise with our interpretation that require attention. The first concern is that there is no significant φ response observed on electrode pairs 2-3 and 3-4 between the zone of bacterial injection and zone of final bacterial accumulation. This is readily explainable by the chemotactic behavior of the bacteria. Nutrients behave as the attractant, so after the nutrients are depleted near the bacterial injection location, the microbes move toward the areas of elevated nutrient concentration at the lower part of the column (fluid inlet). This microbial movement likely occurs gradually (rather than as a bulk movement of the bacterial zone down the column). We assume that the concentration of bacteria swimming from the injection zone towards the inlet at any one time is insufficient to cause a phase anomaly similar to that observed at the injection and final accumulation sites. Thus a measurable IP effect is observed only at the zone of high initial bacterial accumulation and zone of later bacterial accumulation. The second concern is associated with the incomplete relaxation of phase shift between electrodes 1 and 2. This residual phase shift is the result of the accumulation of sulfide precipitates near the base of the column, which presumably extends beyond the limits of the area measured by this electrode pair.

Conclusion

We have presented results of electrical measurements during microbial-mediated metal sulfide precipitation in sand columns. The temporal response of IP measurements suggests sensitivity to the temporal microbial processes occurring in the columns. Most significantly, IP measurements show a spatiotemporal behavior that correlates very closely with the rate of lactate consumption observed within the columns. This raises the intriguing possibility of using IP measurements as non-invasive proxy indicators of microbial metabolism and cell respiration or/and as locators of microbial movement pathways.

Acknowledgements

REFERENCES

Angoran, Y. and T. R. Madden (1977). "Induced Polarization: A Preliminary Study Of Its Chemical Basis." Geophysics **42**(4): 788 - 803.

Archie, G. E. (1942). "The electrical resistivity log as an aid in determining some reservoir characteristiscs." Transactions of the American Institute of Mining, Metallurgical, and Petroleum Engineers **146**: 54-62.

Labrenz, M., et al. (2000). "Formation of Sphalerite (ZnS) Deposits in Natural Biofilms of Sulfate-Reducing Bacteria." Science Magazine **290**.

Madigan, M. T., et al. (1997). Brock biology of microorganisms. Upper Saddle River, NJ, Prentice Hall.

Marshall, D. J. and T. R. Madden (1959). "Induced Polarization, A Study Of Its Causes." Geophysics **XXIV**(4): 790 - 816.

Pelton, W. H., et al. (1978). "Inversion of Two - Dimensional Resistivity and Induced Polarization Data." Geophysics **43**(4): 788-803.

Slater, L. D. and D. Lesmes (2002). "Electrical - hydraulic relationships observed for unconsolidated sediments." Water Resources Research **38**(10).

Sumner, J. S. (1976). Principles of Induced Polarization for Geophysical Exploration. Amsterdam - Oxford - New York, Elsevier Scientific Publishing Company.

Vanhala, H. (1997). "Mapping oil contaminated sand and till with the spectral induced polarization method." Geophysical Prospecting **45**: 303-326.

Vanhala, H. and H. Soininen (1995). "Laboratory technique for measurement of spectral induced polarization response of soil samples." Geophysical Prospecting **43**: 655-676.

Wong, J. (1979). "An electrochemical model of the induced-polarization phenomenon in disseminated sulfide ores." Geophysics **44**(7): 1245-1265.

Figure 1

Active parallel columns for (a) electrical and (b) geochemical measurements. Electrode locations, sampling points, fluid inlet, fluid outlet, zone of bacterial injection and zone of final bacterial accumulation are also shown.
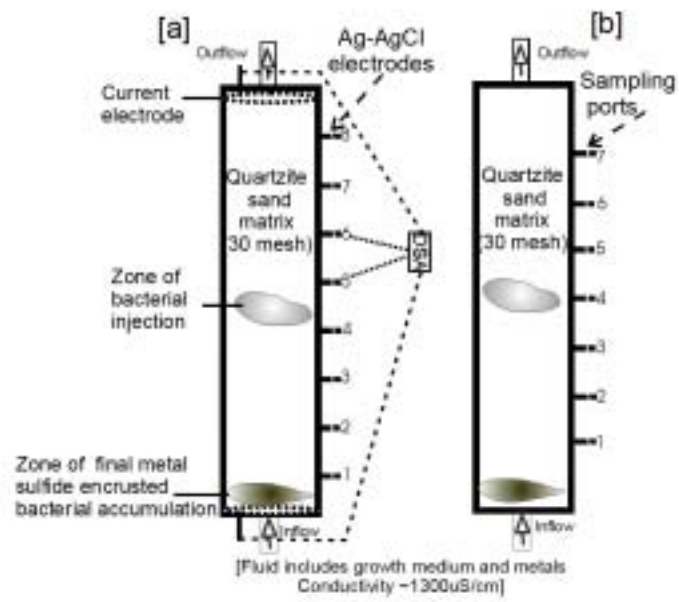
Figure 2

[a] Electrical column showing electrode pairs where measurements are plotted and a conceptual view of the assumed chemotactic movement of bacteria [b] Conductivity magnitude ($|\sigma|$) and phase (φ) response observed between electrode pairs 1-2, 3-4, 4-5 and 6-7 at 35Hz.
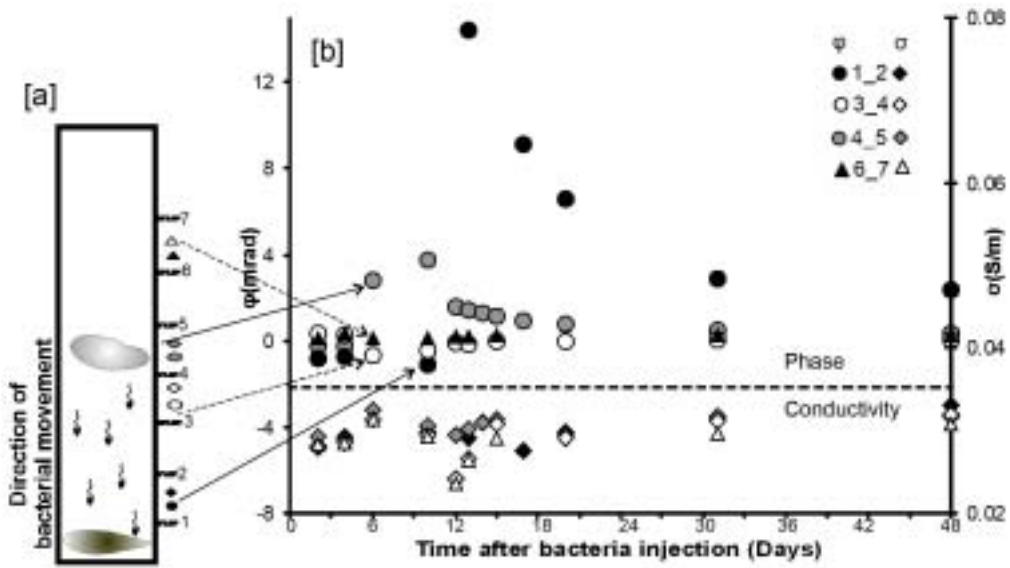
Figure 3

SEM images of samples obtained from two locations within the column. [a] Single microbial cell encrusted with sulfide nodules from region near electrode pair 6-7; and [b] quartz grain encrusted with a thick layer of metal-sulfide coated bacterial cells forming a biofilm from a region below electrode pair 1-2.
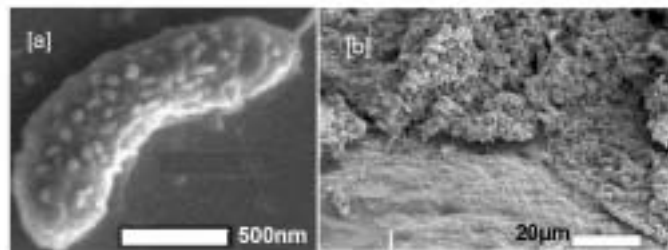
Figure 4

Geochemical data showing [a] the sulfate and lactate concentration over time in sampling ports 1 and 5; and [b] the gradient of lactate concentration over time at the zone of microbial injection and the zone of final microbial accumulation correlated with the φ response observed in electrode pairs 4-5 and 1-2.
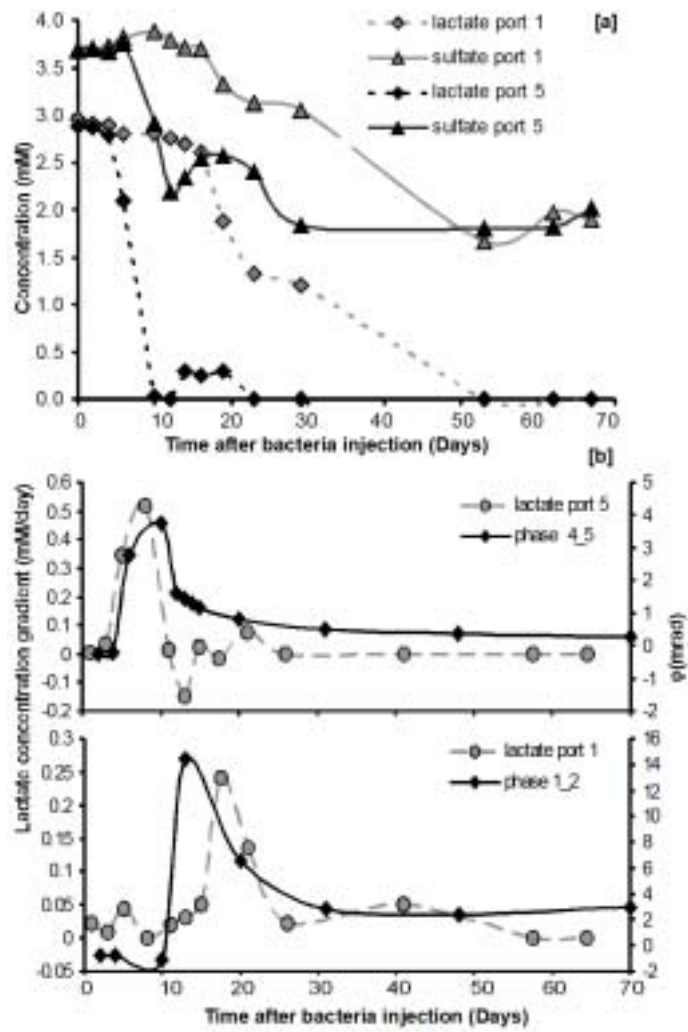
[a]

Outflow

Ag-AgCl electrodes

Current electrode

Quartzite sand matrix (30 mesh)

8

7

6

Zone of bacterial injection

5

4

3

2

Zone of final metal sulfide encrusted bacterial accumulation

1

Inflow

[b]

Outflow

Sampling ports

Quartzite sand matrix (30 mesh)

7

6

5

4

3

2

1

Inflow

[Fluid includes growth medium and metals
Conductivity ~1300uS/cm]

Ntarlagiannis et al. Figure 1

Ntarlagiannis et al. Figure 2

Ntarlagiannis et al. Figure 3

Ntarlagiannis et al. Figure 4